



PREPARATION AND MODELING (TITANIUM-HYDROXYAPATITE) FUNCTIONALLY GRADED MATERIALS FOR BIO-MEDICAL APPLICATION

Dr. NabaaSattar Radhi

Babylon University/Collage of Materials Engineering
Babil/Iraq

ABSTRACT

The composite materials were appeared and using widely in many applications specially in the biomedical field and this materials were improved the life quality since hundreds years ago. In this research prepared functionally graded samples multi layers of (100% Titanium-50%Titanium-50% Hydroxyapatite-100% Hydroxyapatite), and prepared each layer singly sample to investigated behaviour of each layer and total functionally graded. In this research test the XRD of powder, density, porosity, particle size analyser and micro hardness. Finally modelling the samples by ANSYS version 15 to calculate the total stress and strain that affect to implant in human body.

Key words: ANSYS, Biomaterials, Biomedical, Functionally graded, Modeling and XRD.

Cite this Article: Dr. NabaaSattar Radhi, Preparation and Modeling (Titanium-Hydroxyapatite) Functionally Graded Materials for Bio-Medical Application, International Journal of Civil Engineering and Technology, 9(6), 2018, pp. 28–39.
<http://www.iaeme.com/IJCIET/issues.asp?JType=IJCIET&VType=9&IType=6>

1. INTRODUCTION

The purpose of biomedical materials are the interfacing with the biological system inside human body in order to assess, remedy, grow up or replacement any live tissue, member function of the body and the planting of these materials can not complete without the Biocompatibility between the new object and the environment inside the body. So, the Biocompatibility is known as the ability of the host to deals with a new planting materials in the specific application and the Host response include: the reaction of a living system to the presence of a material (Al-hydary, 2010 and K.N. Kadhim and Ahmed H. 2018).

1.1. Titanium

Titanium is one of the metals that has the highest strength/weight ratio and the highest corrosion resistance compared with other metals. For the previous reason in addition to the non-magnetic characteristics for this metal, Titanium is used in many application such as

bone-fracture fixation in spinal fusion devices, pins, bone-plates and screws. Because the magnetic characteristics have bad impact and threatening the human life during the magnetic resonance imaging (RIM) and exposure to electronic equipment. As well as, Titanium is used in surgical instruments production because Titanium does not effected by corrosion or loosing of surface properties by repeating sterilization also the light weight of this metal will reduce surgeon tiredness during the operations, (Vincent, 1999).

1.2. Hydroxyapatite: Structure and Characteristics

Hydroxyapatite (HA) one of the famous ceramic materials that considered bioactive and used in medical field specially in bones. [(Al-hydary, 2010) and (Narayan, et.al., 2004)]. The non-live bones consists of biological apatite to give bone the required strength and it work as calcium, phosphorus, sodium, and magnesium storage.

HA forms by hexagonal rhombic prisms crystals The lattice parameters for hydroxyapatite are $a=9.432 \text{ \AA}$ and $c=6.881 \text{ \AA}$. Hydroxyl ions (OH^-) occur at the corners of the basal plane. Ions are located at every 3.44 \AA (half-cell), which is perpendicular to the plane of basal and in parallel to the c-axis. So, in unit cell about 60% of calcium ions are linked with the hydroxyl ions. The density of this material is 3.219 g/cm^3 , (Park, 1992 and K.N.Kadhim et al.2016). Consequently, conventionally processed HA demonstrates poor chemical and thermal stability, and decomposes when densified at high temperatures [(Akao, et.al., 1981) and (Ruys, et.al., 1995)].

1.3. Literature Survey

Pt/HA Nanocomposites

Estrada, et.al., 2006, described a method for incorporating ductile platinum particles into a hydroxyapatite matrix in order to improve the fracture toughness. They determined the effect of volume fraction of platinum particles on the fracture toughness and compared the results with predictions based on models in the literature. They measured the fracture toughness of the composite using a Vickers indentation technique. The results indicated that the incorporation of the particles improved the measured fracture toughness of the composite in a manner consistent with that predicted in the literature.

Ti/HA Nanocomposites

Estrada et. al. 2006, studied the improvement in the mechanical characteristic of HA by coating its surface with Ti nanoparticles in sizes from 8 to 70 nm through the deposition of Ti by laser ablation. A comparison of the hydroxyapatite hardness before and after deposition was performed using scanning probe microscopy (SPM) nano-indentation. Based on TEM observations, they showed that the Ti nanoparticles obtained were covered by an oxygen shell and the nanoparticles were deposited on the irregular surface of HA producing a smoother morphology and covering totally the ceramic.

Simon et.al., 2005. considered a new system of functionally graded materials consist of titanium with HA. They obtained the samples by sintering titanium with HA powders. The bioactivity was tested in simulated body fluid (SBF). The sintering conditions lead to convenient values of samples density as compared with bone density. The size of HA developed at the sample surface after soaking for a week in SBF is about hundreds of micrometers, depends on the pressing force applied during sintering process, and tend to form a continuous network of the new developed bioactive layer indicating that these materials proved to have bioactive behaviour.

2. DESIGN AND MODELLING

A model is a symbolic terms built to simulate and predict aspects of behaviour of a system. The rapidly increasing performance of computers and computer software has favoured the widespread use of numerical simulation tools for the design of parts and for the optimization of manufacturing processes. Modelling may be especially important in connection with functionally graded materials, since the gradients often cause special problems, (Markworth, et.al., 1995).

2.1. Modelling of Functionally Gradient Materials (FGMs)

Mixture rules are represented in the work of Wakashima et al. They considered a material having two components, one is hydroxyapatite and the other is titanium, denoted as *HAP* and *Ti* respectively. Let P_{HAP} and P_{Ti} be the values of any special characteristic for pure HAP and pure Ti in that order, and let their respective volume fractions be V_{HAP} , eq.(1) and V_{Ti} be in eq.(2). The famous Voigt –type guess for effective value P of this characteristic (Markworth, et.al., 1995).

A Model used after Wakashima et al, which is expressed as:

$$V_1(z) = \left(\frac{Z_2 - Z}{Z_2 - Z_1} \right)^N \dots\dots\dots(1)$$

Where:

$V_1(z)$: is the local volume fraction of phase1, the volume fraction of phase2 being:

$$V_2(z) = 1 - V_1(z) \dots\dots\dots(2)$$

(Z_1) and (Z_2) are border regions of pure phase 1 and phase 2, respectively.

Z : is the distance from (layer1) to (layer3) and exponent (N) is a variable parameter.

$$[P = P_{HAP} V_{HAP}(z) + P_{Ti} (1 - V_{HAP}(z)) \dots\dots\dots(3)]$$

2.2. Steps of FEM

The chief stages of a FEM analysis described in relation to a specimen issues: the loading of an implant for the duration of standing up. To look for the displacements in the implant and for the stresses in the bone holding the prosthesis, (Ansys-11, 2008).

2.2.1. Pre-processing

To starting the components analysis, the element should draw firstly, and due to FEM software isn't designed for drawing usage, so Solid model or CAD was used to performed the task. The solid model could be chosen for drawing and then imported into the FEM software, (Ansys-11, 2008). Figure (1,a). shows an example for chosen this software.

2.2.2. Selected Element

In ANSYS library there are more than one hundred element types that differ in a unique number and a prefix that classified the element group. In this research (SOLID-8 Brick 185) was used to producing (3-D modelling) for solid structures, (Ansys-11, 2008).

2.2.3. Material Properties

The mechanical properties (Tensile strength and Young's modulus) of the HAP and Ti materials used in this work are determined from tensile test and (Poisson's ratio and density) were calculated theoretically by the Rule of mixture [(Consolo, et.al., 2010) and (Ahmed, 2011)]. Table (1) contains tensile properties and densities of three layers alloy used in this work.

Table 1 Tensile Properties and Densities for materials used in this work.

Layers	Composition (wt %)	Thickness (mm)	E(GPa)	Poisson's Ratio	Density (g/cm ³)
1 st	100% Ti	3	116	0.32	4.5
2 nd	50% Ti-50% HAP	3	83	0.31	3.8595
3 rd	100% HAP	3	50	0.3	3.219

2.2.4. Mesh Generation

The implant as previously stated, is a very complex, layered composite structure, and the first step of the finite element analysis is to discretize the structure into finite elements connected at nodes. For a structure, as an implant, it is necessary to discretize it into a sufficient number of elements in order to obtain a reasonable accuracy, (Higgs, 2002). The mesh generation of implant is as shown in figure (1,b).

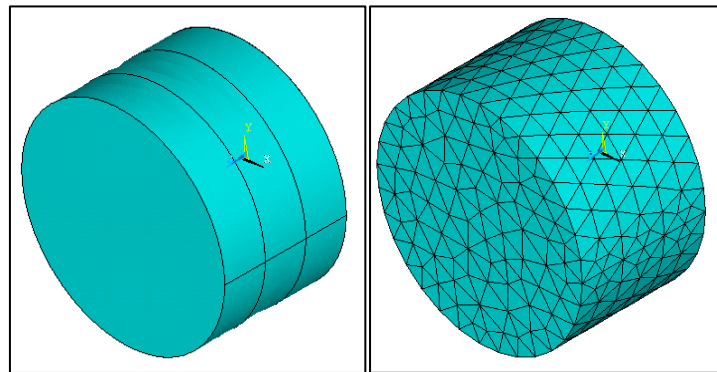


Figure 1 Draw three layers Ti-Hap FGM as an implant for

a: Draw three layers. b: Meshing FGM.

2.2.5. Loading and Boundary Conditions

The main aim of using finite element analysis is to study the responds of each element for each loading condition. In ANSYS terminology, the word (loads) include the boundary condition and either external or internal force functions that applied like displacements, forces, pressure and gravity in structural disciplines. [(Zulkifli, et.al., 2011) and (Callisterand Rethwisch, 2007)].

2.2.6. Solution of the System Equations

In this step, the global system of equations is solved to obtain the unknown field variables. There are number of solution schemes available depending on the problem size (number of degrees of freedom), available computer storage, type of the system of equations (symmetric or not), etc. The most common solution schemes are the skyline scheme, the frontal solution scheme and iteration schemes, (Bolten, 1998).

Displacement

Displacement (extension and contraction) along the model as a result of loading (human weight) is represented in figures (2) presents the values of displacement versus (Z) distance along the three layers of prepared FGMs. Thus, the values of displacement at any point along the model can be determined. At FGM the maximum displacement (i.e. Expansion) can be found at the surface of a third layer alloy of about $(0.3277e^{-6}$ mm) as indicated in figure (2), then decreases along the layers of the sample with noticeable fluctuation.

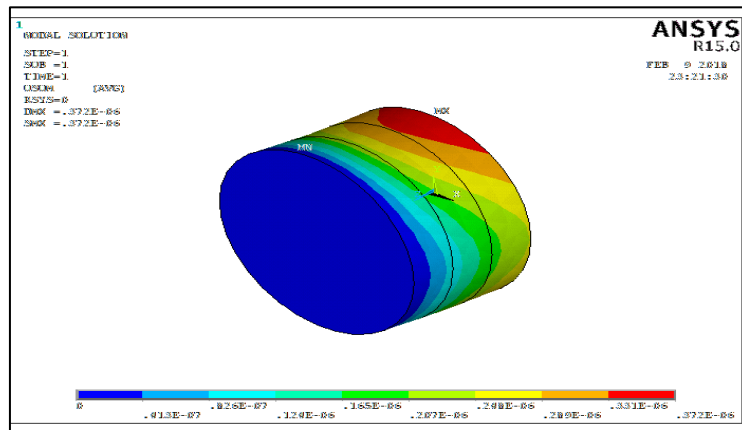


Figure 2 Contour of displacement FGM 3-D.

Von Misses stress

Von Misses stresses have been represented in figure (3) represent values of residual stresses versus (z) distance from first layer alloy to third layer. In a conclusion, interesting remarks will be seen as the results of residual stresses that develop along with the model. The maximum stresses are concentrated on the third layer alloy and the positive value of residual stresses at 687N for FGM around 0.275 MPa. All of these residual stresses results are assumed to be acceptable from the design point of view since they do not exceed 450 and 50 MPa the value of yield strength of Ti and HAP, (Mitchell, 2004).

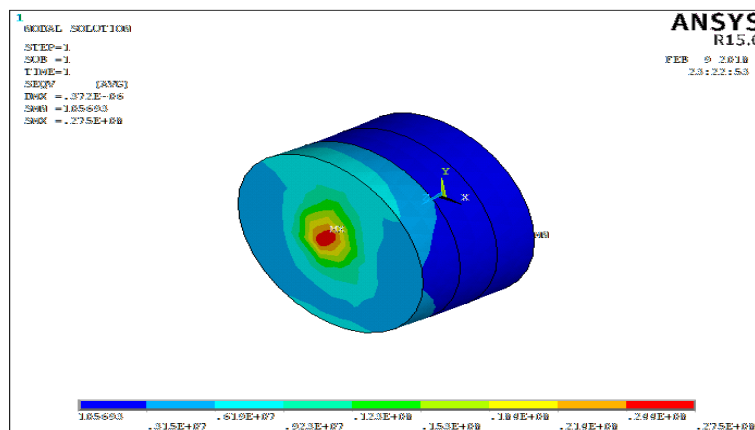


Figure 3 Contour of Von Misses stress FGM 3-D.

Von Misses strain

Von Misses strains have been represented in figure (4) represent values of Von Misses strains versus (z) distance from first layer alloy to third layer alloy. In a conclusion, interesting remarks will be seen as the results of Von Misses strains that develop along with the model. The maximum strains are concentrated on the first layer and the positive value of strain for Ti-HAP FGM around 2.5×10^{-6} at 687N stresses that develop are less than 2.37×10^{-4} .

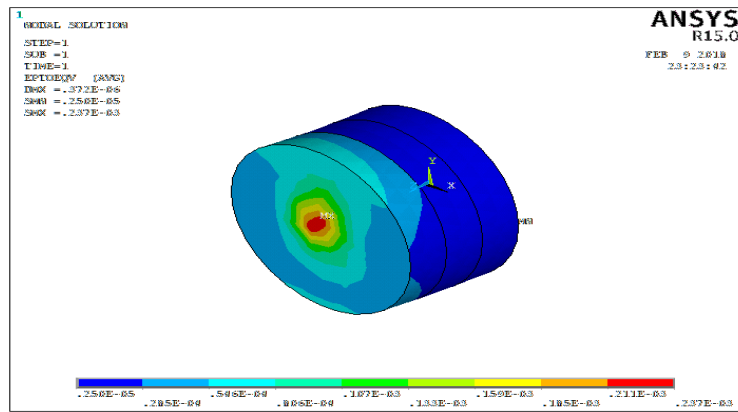


Figure 4 Contour of Von Misses strain FGM 3-D.

3. EXPERIMENTAL PART

This section involves the materials and equipment that are used in this work, and the sequence of operations and tests that have been accomplished. And the base alloy which used in this work are Titanium and hydroxyapatite powder, all the above powders should be of high purity (99.9 wt %) because they are for human use, and any undesirable elements may cause side effects on the human health. The materials that used in this work are:

- High purity Titanium powder of 98.5 wt%, which was analyzed by XRD.
- Hydroxyapatite has the purity of 99.9 wt%, which was analyzed by XRD.

The elemental powders (i.e. HA and Ti powder) used in this research to prepare several FGMs layers with an average particle size, purity and origin are shown in table (2).

Table 2 Powders used in this study.

Powder	Average particle size(μm)	Purity %	Origin.
Hydroxyapatite	33	99.8	BDH Chemicals Ltd Poole England
Titanium	165	98.5	Fluke Chemi AGCH-9470 Bucks

3.1. Plan of work

The plane of work can be explained as following:

- Preparation of FGM layers indicated in table (3).
- Wet mixing of the powders for 2 hours.
- Filling of powders into the die cavity by stepwise controlled manner.
- Compacting of powders with pressure 300 MPa.
- Sintering of all prepared samples in furnace at 950°C at 7 hours.
- Measuring of apparent density, porosity.
- Hardness testing along the thickness of the prepared samples to examine the gradation of properties along the thickness.
- Using X-Ray Diffraction (XRD) to detect phases that developed during sintering.

Table 3 Model of FGM profile

Layers	Chemical composition	Thickness (mm)
1 st	(100% wtTi)	3
2 nd	(50% wt Ti-50% wt HA)	3
3 rd	(100% wt HA)	3

3.2.2. Apparent density of powders and blended powders

Apparent density determinations are made by pouring powder into standard graded cub with 10 ml maximum volume into suitable grade. During the work must take care of the powder to prevent physical densification in the cup when levelling. Weight of cup with and without powder is calculated using microbalance with an accuracy of (± 0.0001 g). Apparent density in g/cm^3 then identified by eq.(4)

$$\rho_A = \frac{m_2 - m_1}{V_p} \quad (4)$$

Where:

- ρ_A = Apparent density of powder (g/cm^3).
- m_1 = weight of cup without powder (unfilled cup (g)).
- m_2 = weight of cup with powder (g).
- V_p = volume of powder in cup (cm^3)

3.2.3. Green porosity and Density

The volume unit weight of compacted blended powder expressed in g/cm^3 is the green density of the compact. It calculates by the dimensions evaluation and the weight of compact specimen as shown in eq.(5):

$$\rho_g = \frac{m_g}{V_g} \quad (5)$$

Whereas:

- ρ_g = green density (g/cm^3).
- m_g = green mass of the compact (g).
- V_g = volume of the compact (cm^3).

The theoretical density is important to determine the Green porosity from blended powders density (mixture) and the Green porosity identified by the percent of the weight for the element powder multiplied by the theoretical density as shown in eq.(6)

$$\rho_{tB} = \sum_{i=1}^n Wt_i * \rho_i + Wt_2 * \rho_2 + Wt_3 * \rho_3 + \dots + Wt_n * \rho_n \quad (6)$$

Whereas:

- ρ_{tB} = theoretical density of blended powder (g/cm^3).
- n = No. of elemental powders.
- Wt_i = weight percent (%).
- $\rho_{1,2,3,\dots,n}$ = density of elemental powder (g/cm^3).

So the green porosity calculates by eq. (7) as shown:

$$P_g = \left(1 - \frac{\rho_g}{\rho_{tB}}\right) \times 100\% \quad (7)$$

Whereas:

P_g = green porosity (%).

ρ_g = green density (g/cm³).

ρ_{tB} = theoretical density of blended mixture (g/cm³).

3.2.4. Microhardness Measurements

This apparatus used to measure hardness with 1000g load and holding time of 20 seconds to the surface of the specimen using a standard 136° Vickers diamond pyramid indenter combined with optical microscopy to measure the diagonal length of Vicker's impression. The Vicker's microhardness (H.V.) is specified as follows (Mitchell, 2004):

$$HV = 1.854P/d^2 \quad (8)$$

Whereas:

P = applied load.

d = average length of diagonal μm .

The three readings are reordered for each sample of layers and ten readings are recorded for functionally graded samples.

4. RESULTS AND DISCUSSION

The experimental results of X-ray diffraction, micro-hardness HA and titanium samples are discussed in detail. The discussion also includes the results of particles size analyzer and green density of compact samples.

4.1. Green Density of Compacts

Green density of compacted specimen is shown in figure (5) with expected pressure. For all samples, green density increases with increasing of the pressing stress, from 233 MPa to 350 MPa. As read from figure (5), as compacting pressure is based for all next studies of all other parameters such as rate of loading, the period of maximum load and all parameters in the sintering process.

Effect of Rate of Loading

To explain effect of rate of loading on the green density of compacts, three rates (0.1, 0.3 and 2.2 kN/sec) have been studied. Figure (6) shows the effect of loading rate on the green density of each layer composition and blended mixtures of powder. It has been shown that increasing rates of loading leads to decrease green density for all blended powders when the rate is slow (0.1 in/sec), there is a period that the powder particles move and slide together so many pores are filled with small particle size.

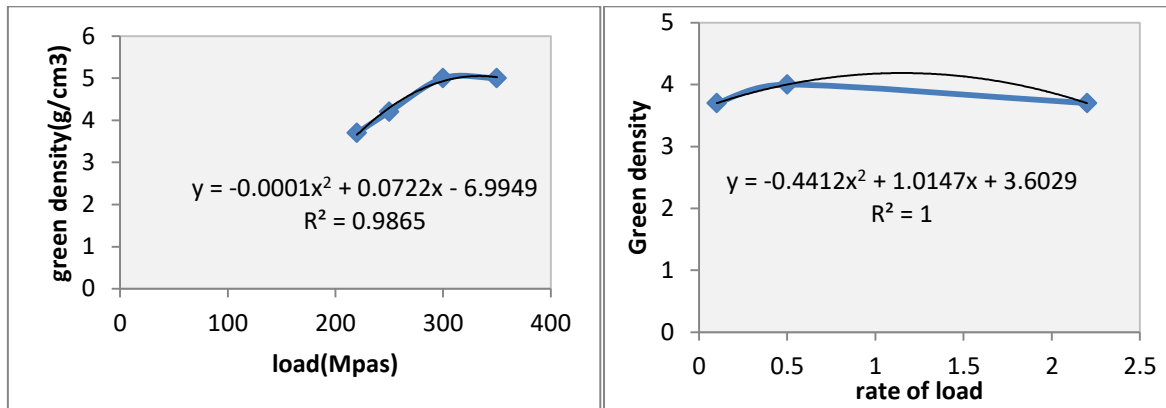


Figure 5 Green density as a function of load. **Figure 6** Green density as a function of rate of loading.

4.2. X-ray diffraction pattern of compacts

X-ray diffraction analyses of powdered form HA and titanium have been studied in order to identify metal powders used in this study as illustrated in figures (7 and 8). X-ray diffraction test was performed on the specimens of HA and titanium powders to investigate the existing phases in each specimen. The diffraction angle is ($2\theta^\circ$) and its range was (20° - 70°) for Ti and (10° - 50°) for HA, the resulting phases are explained below. Figure (7) Illustrates X-ray diffraction results for HA powder. While Figure (8) Illustrates X-ray diffraction results for titanium sample.

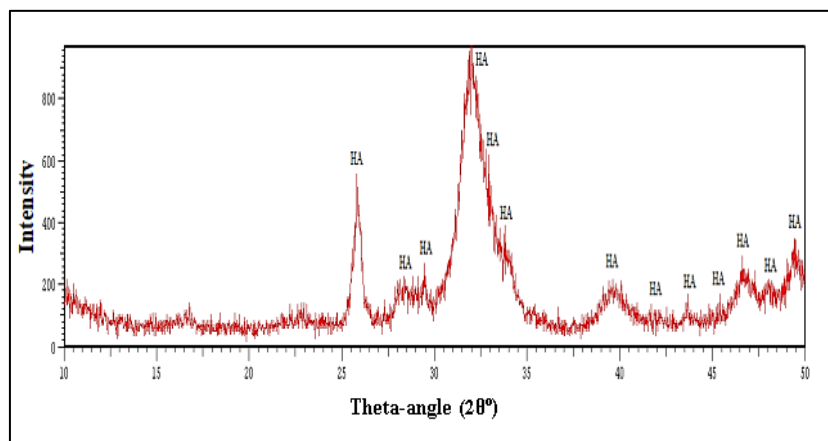


Figure 7 XRD pattern of HA powder.

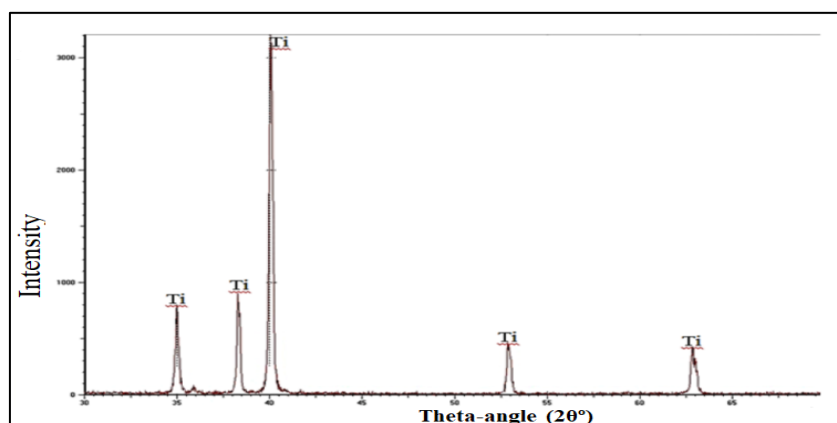


Figure 8 XRD pattern of titanium powder.

4.3. Micro-Hardness Measurement

The micro-hardness measurements have been made for the samples produced by powder metallurgy approach (compaction and sintering) by taking the average of 5 readings at each point while the functionally graded samples by taking the average of 10 readings. The hardness values for these samples were taken from longitudinal and transverse directions while functionally graded samples the hardness values were taken at longitudinal directions in order to study the influence of the mechanical working. The outcomes obtained are represented graphically in figure (9) and table (4).

Table 4 Shows the value of micro-hardness test.

Samples	Value of microhardness (kg/mm ²)
1 st layer(Ti)	412
2 nd layer(Ti-HAP)	517
3 rd layer (HAP)	745
FGM(Ti-HAP)	630

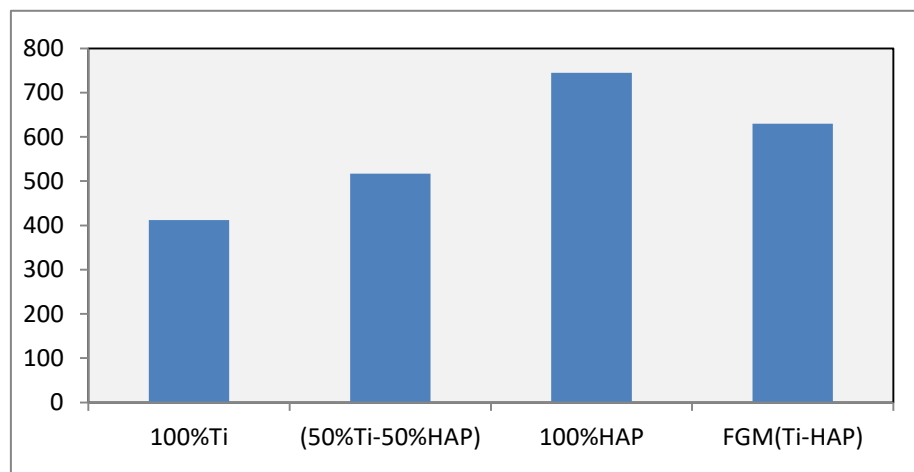


Figure 9 Show the micro-hardness of functionally graded samples with thickness.

Figure(9) shows that the measured hardness value for the functionally graded samples. It is known that the HA is harder and more brittle than Ti i.e. the latter is stronger and softer in this system, (Abid-Ali, 2008) and as the samples consists of HA and Ti, it is concluded (from the hardness values) that the amount of the HA is more than that of the Ti one. Therefore, it might also be judged that a purely HA phase would have a higher hardness value. (which is considered to have higher strength).

5. CONCLUSIONS

Depending on the experimental results, the following deductions may be described:

- Design of three layered functionally graded materials was proposed to ensure a linear variation of constituents (i.e. HAP& Ti) along the layers.
- The sintering at (950°C±5) for (7 hrs.) of prepared samples seems to be real effective to satisfy sintering completely HAP and Ti into structure which obtained.
- The HAP-Ti prepared resulted in decreasing the hardness relatively with increasing titanium content while the FGM samples decreased to core or increased dependent totitanium content.
- The maximum displacement (i.e. expansion) can be found at the surface of third layer alloy and gradually then decreases along the layers of the sample with noticeable fluctuation.

Preparation and Modeling (Titanium-Hydroxyapatite) Functionally Graded Materials for Bio-Medical Application

- The maximum stresses are concentrated on the third layer alloy and the positive value of residual stresses at 687N for FGM 6.461 MPa
- The maximum strains are concentrated on the third layer alloy and the positive value of strain for FGM.

REFERENCES

- [1] Al-Hydary, I., 2010. 'Microstructure and Engineering Properties of Nanocomposites Containing Hydroxyapatite. Ph.D thesis, Post Graduate Department of Materials Science, Sardar Patel University, Vallabh Vidyanagar, Gujarat (India).
- [2] Vincent J.F.V., 1999. Strength and fracture of glasses", *J. of Mat.Sc.*q,26:pp.1947-1950.
- [3] Narayan, R.J., Kumta, P.N., Sfeir, C., Lee, D.H., Choi, D. and Olton, D., 2004. Nanostructured ceramics in medical devices: applications and prospects. *Jom*, 56(10), p.38.
- [4] Park, J.B., 1992. *Lakes, Biomaterials: An Introduction*. Plenum Press, New York.
- [5] Akao, M., Aoki, H., Kato, K., and Mat, J., 1998. *Sci.*, 16:809.
- [6] Ruys, A.J., Wei, M., Sorrell, C.C., Dickson, M.R., Brandwood, A. and Milthorpe, B.K., 1995. Sintering effects on the strength of hydroxyapatite. *Biomaterials*, 16(5), pp.409-415.
- [7] Estrada, J.R.D., Camps, E., Alarcon, L.E. and Ascencio, J.A., 2006. *J Master Sci*, DOL10.1007/S10853-006-1216-Z.
- [8] Simon, V., Muresan, D., Popaa, C. and Simon, S., 2005. *Journal of Optoelectronics and Advanced Materials* Vol.7, No.6, pp.2823-2826, December.
- [9] Markworth, A.J., Ramesh, K.S. and Parks, W.P., 1995. Modelling studies applied to functionally graded materials. *Journal of Materials Science*, 30(9), pp.2183-2193.
- [10] Ansys-11, 2008. *Wokbench help guide*, SAS IP, Inc., Eleventh Edition.
- [11] Consolo, F., Mastrangelo, F., Ciardelli, G., Montevecchi, F.M., Morbiducci, U., Sassi, M. and Bignardi, C., 2010. Multilevel experimental and modelling techniques for bioartificial scaffolds and matrices. In *Scanning Probe Microscopy in Nanoscience and Nanotechnology* (pp. 425-486). Springer, Berlin, Heidelberg.
- [12] Jones, R.M., 1975. *Mechanics of Composite Material*. McGraw-Hill, New York, (1975).
- [13] Kadhim Naief Kadhim and Ahmed H. (Experimental Study Of Magnetization Effect On Ground Water Properties). *Jordan Journal of Civil Engineering*, Volume 12, No. 2, 2018
- [14] Kadhim Naief Kadhim and Ghfrun A. (The Geotechnical Maps For Gypsum By Using Gis For Najaf City (Najaf - Iraq) (IJCIET), Volume 7, Issue 44, July-August 2016, pp. 329–338
- [15] Ahmed, P.S., 2011. *Fatigue Characteristics of Trans-Tibial Prosthetic Socket*. Ph.D. thesis, University of Technology, Department of Materials Engineering, Baghdad.
- [16] Higgs, D., Sanders, P. and Singh, Y.P., 2002. Design Specifications of Lower Limb Prosthesis Socket. In *Proceedings of the ASEE Gulf. Southwest Annual Conference*.

- [17] Bolten, W., 1998. Engineering Materials Technology. Third edition, Butterworth & Heinemann publishing Ltd.
- [18] Zulkifli, A., Ariffin, A.K. and Rahman, M.M., 2011. Probabilistic finite element analysis of vertebrae of the lumbar spine under hyperextension loading. International Journal of Automotive and Mechanical Engineering, 3(1), pp.256-264.
- [19] Callister, W.D. and Rethwisch, D. G., 2007. Materials science and engineering. Seventh edition. Jone Wiley and Sons.
- [20] Mitchell, B.S., 2004. An introduction to materials engineering and science for chemical and materials engineers. John Wiley & Sons.
- [21] Abid-Ali,A.Raheem K., 2008. Investigation of Certain Shape Memory Alloys In Space Systems.Ph.D thesis, Department of material engineering/College of engineering, University of Babylon–Iraq.